Downloaded 09/12/17 to 155.101.18.153. Redistribution subject to SEG license or copyright; see Terms of Use at http://library.seg.org/

Joint inversion of seismic and gravity gradiometry data using Gramian constraints

Wei Lin[1], and Michael S. Zhdanov[1,2,3]*
[1]University of Utah; [2]TechnoImaging; [3]MIPT

Summary

This paper develops a method of joint inversion of seismic and gravity gradiometry data based on the concept of a Gramian stabilizer, which enforces the linear relationships between the different model parameters and their attributes or transforms. We take into account the existence of empirical linear relationships between the log density and log seismic velocity according to Gardner's equation, and use this relationship in the construction of the corresponding Gramian stabilizer. At the same time, the developed algorithm does not require a priori knowledge of the specific parameters of the correlation between the density and velocity, and instead provides the means to find these parameters from the inversion without actual measurement of the physical properties of the rock samples. The developed algorithm of joint inversion is based on modeling the seismic responses using the integral equation (IE) method. The regularized inversion involves minimization of the Tikhonov parametric functional with a Gramian stabilizer using the regularized conjugate gradient method.

Introduction

Seismic imaging is primarily based on the depth migration, which requires an accurate 3D velocity model for accurate time-to-depth conversion. Modern advances in full waveform inversion still meet significant difficulties related to the nonuniquness of the inversion, especially in the presence of high-velocity salt structures. Additional geophysical fields provide information about different physical properties of the subsurface. For example, there are significant contrasts in the physical properties of salt structures and host rocks for gravity and electromagnetic (EM) measurements. When combined with seismic, these methods can be integrated in a shared earth model and interpreted for geology. Ultimately, a velocity model must be delivered for reprocessing of the seismic depth migration/inversion images. However, the question remains how to "integrate" these fundamentally different data for self-consistent 3D earth models of their respective physical properties.

To this end, Zhdanov et al. (2012a) introduced a unified approach to joint inversion using Gramian constraints. These Gramian constraints are based on the minimization of the determinant of the Gram matrix of a system of different model parameters or their attributes (i.e., a Gramian). The underlying idea of this approach is that the Gramian provides a measure of correlation between the model parameters and/or their attributes. By imposing an additional requirement of minimizing the Gramian during the regularized inversion, one recovers multiple models with enhanced correlation between the different physical properties and/or their attributes.

Joint inversion of seismic and gravity data based on the Gramian constraint

Consider two different geophysical data sets:

$$\mathbf{d}^{(i)} = [d_1^{(i)}, d_2^{(i)}, \dots, d_{N_d}^{(i)}]^T, i = 1,2, \quad (1)$$

representing gravity and seismic data, respectively, and the related two physical properties,

$$\mathbf{m}^{(i)} = [m_1^{(i)}, m_2^{(i)}, \dots, m_{N_m}^{(i)}]^T, i = 1,2, \quad (2)$$

representing velocity (v) and density (ρ), respectively.

We can describe the modeling of two geophysical data sets as the operator relationships:

$$\mathbf{d}^{(i)} = \mathbf{A}^{(i)}(\mathbf{m}^{(i)}), i = 1,2, \quad (3)$$

where $\mathbf{A}^{(1)}$ and $\mathbf{A}^{(2)}$ are the operators of seismic and gravity forward modeling, respectively.

In the case of a joint inversion of the seismic and gravity data, one can use an empirically derived equation that relates seismic P-wave velocity, v, and the bulk density, ρ. For example, Gardner's equation can be applied (Gardner et al., 1974):

$$\rho = f(v) = kv^l, \quad (4)$$

which is widely used in oil and gas exploration because it provides information about the lithology from interval velocities obtained from the seismic data. In the last formula, the constants, *k* and *l*, can be derived from seismic and density well log information.

In many practical situations, we do not have a priori knowledge about a specific form of functional relationships between the different properties (model parameters). In this case, one can use a more general approach to joint inversion of multimodal geophysical data using Gramian constraints, which are based on the minimization of the determinant of a Gram matrix of a system of different model parameters or their attributes (Zhdanov et al., 2012a, b). The method does not require any a priori knowledge about the types of relationships between the different model parameters, but instead determines the form of these relationships in the process of the inversion. For example, in a case of using Gardner's relations between the seismic velocity and density, equation (4), we may not always know exactly the values of Gardner's parameters, *k* and *l*. However, formula (4) shows that the logarithm of density is linearly related to the logarithm of velocity:

$$\ln(\rho) = k + l \cdot \ln(v) \quad (5)$$

Thus, we can develop the method of joint inversion, which enforces the linear correlation between $\ln(\rho)$ and $\ln(v)$.

© 2017 SEG

Downloaded 09/12/17 to 155.101.18.153. Redistribution subject to SEG license or copyright; see Terms of Use at http://library.seg.org/

The joint inversion for these two model parameters can be formulated as a minimization of a single parametric functional according to the following formula (Zhdanov et al., 2012a, b; Zhdanov, 2015):

$$P^{\alpha}\left(\mathbf{m}^{(1)},\mathbf{m}^{(2)}\right)=\sum_{i=1}^{2}\varphi^{(i)}(\mathbf{m}^{(i)})+\sum_{i=1}^{2}\alpha^{(i)}S_{MN}(\mathbf{m}^{(i)})+\beta S_G(TL\mathbf{m}^{(1)},TL\mathbf{m}^{(2)}). \quad (6)$$

where the coefficients $\alpha^{(i)}$ and β are some positive numbers introduced for weighting the different parts of the parametric functional; the misfit functionals, $\varphi^{(i)}$, are given by the following formula:

$$\varphi^{(i)}=\left\|\mathbf{W}_d^{(i)}\left(\mathbf{A}^{(i)}\left(\mathbf{m}^{(i)}\right)-\mathbf{d}^{(i)}\right)\right\|^2, i=1,2, \quad (7)$$

and the minimum norm stabilizing functionals, S_{MN}, are calculated as follows:

$$S_{MN}^{(i)}=\left\|\mathbf{W}_m^{(i)}(\mathbf{m}^{(i)}-\mathbf{m}_{apr}^{(i)})\right\|^2, i=1,2, \quad (8)$$

where $\mathbf{W}_d^{(i)}$ and $\mathbf{W}_m^{(i)}$ are the data weighting and the model weighting matrices; and the term S_G is the Gramian constraint, which in a case of two physical properties can be written, using matrix notations, as follows:

$$S_G=\begin{vmatrix}(TL\mathbf{m}^{(1)},TL\mathbf{m}^{(1)}) & (TL\mathbf{m}^{(1)},TL\mathbf{m}^{(2)})\\ (TL\mathbf{m}^{(2)},TL\mathbf{m}^{(1)}) & (TL\mathbf{m}^{(2)},TL\mathbf{m}^{(2)})\end{vmatrix}, \quad (9)$$

where operator L represent some log transformation of the model parameters; and operation $(\cdot,\cdot)$ stands for the inner product of two vectors in the corresponding Gramian space. The choice of operator T is important in determining the form of correlation between the model parameters, $\mathbf{m}^{(1)}$ and $\mathbf{m}^{(2)}$. In this study, we choose operator T as follows:

$$T\left(\mathbf{m}^{(i)}\right)=\mathbf{m}^{(i)}-\frac{\sum_{j=1}^{N_m}m_j^{(i)}}{N_m}, i=1,2. \quad (10)$$

One of the important characteristics of the operator T is that $T(k)=0$ if the argument, k, is a constant. Thus we can arrive at the following relation between the logarithm of density and velocity:

$$TL(\rho)=T(k+l\cdot\ln(v))=l\cdot TL(v). \quad (11)$$

In some circumstances, we would like to constrain the inverted parameters within the given boundaries, $[m_{\min}^{(i)},m_{\max}^{(i)}]$. These constraints can be implemented replacing the original parameters, $\mathbf{m}^{(i)}$, with the new parameters, $\mathbf{x}^{(i)}$:

$$\mathbf{x}^{(i)}=[x_1^{(i)},x_2^{(i)},\dots,x_{N_m}^{(i)}]^T, i=1,2, \quad (12)$$

where

$$m_k^{(i)}=\frac{m_{\max}^{(i)}e^{x_k^{(i)}}+m_{\min}^{(i)}}{e^{x_k^{(i)}}+1}, \begin{cases} i=1,2\\ k=1,2,\dots,N_m\end{cases}. \quad (13)$$

As a result, the inversion should be run for the new model parameter, $\mathbf{x}^{(i)}$.

We use the regularized conjugate gradient method (Zhdanov, 2002) to minimize the parametric functional (6).

The efficiency of any inversion method is determined first of all by the corresponding forward modeling algorithm. The gravity forward modeling is straightforward and has been discussed in many publications, (e.g., Zhdanov, 2002, 2015). The seismic forward modeling is based on the method of integral equations (IE) (e.g., Aki and Richards, 1980; Bleistein, 1984; Zhdanov, 2002, 2015).

Numerical study of the joint inversion of seismic and gravity data for 3D SEG model

Model 1

In this section, we present the results of the joint inversion of seismic and gravity data using a 3D synthetic model formed by an anomalous body with a density of 2.19 g/cm^3, and a velocity of 2500 m/s, where the background density and velocity are 2.61 g/cm^3 and 5000 m/s, respectively. The size of the body is 400 m×400 m×200 m, where the depth of the top of the body is 200 m. The synthetic correlation between the densities ρ and velocity v is described by Gardner's equation (4) with (k, l) = (0.31, 0.25).

We have assumed that the observed data for this model were the full tensor gradiometry (FTG) data and the seismic wave responses. The FTG components used in this synthetic study were G_{zz}, G_{zx} and G_{zy}. The synthetic source term for seismic forward modeling was the Ricker wavelet with the peak frequency of 20 Hz. Figure 1 shows the synthetic source positions (red dots) and receiver positions (blue crosses). The spacing between adjacent receivers was 10 m. In this synthetic study, we chose three frequencies for the observed seismic data: 1 Hz, 5 Hz, and 10 Hz. The synthetic seismic and gravity data were both contaminated by 1% Gaussian noise.

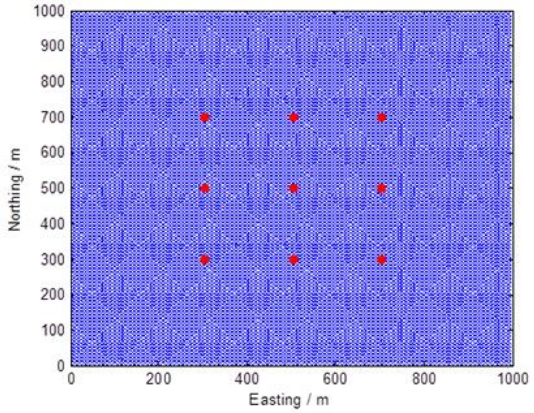

Figure 1: Model 1. Plan view of the seismic source (red dots) and receivers (blue dots) configuration.

We first ran separate inversions for seismic and gravity data, respectively. The iterative inversion process was terminated when the normalized misfit reached 1%. Figure 2 shows the recovered velocity and density distributions, and the white boxes outline the true location of the anomalous body. While the gravity inversion produced a diffused anomalous density distribution, the seismic

© 2017 SEG

Downloaded 09/12/17 to 155.101.18.153. Redistribution subject to SEG license or copyright; see Terms of Use at http://library.seg.org/

inversion recovered the anomalous body at its true location and with the correct values of the velocity. This could be explained by a very dense grid of the seismic receivers and overall high resolutions of seismic method.

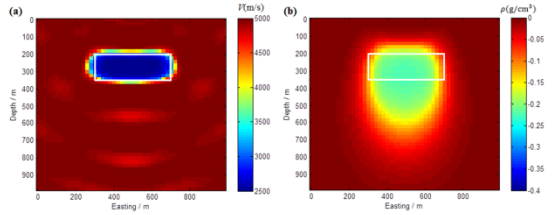

Figure 2: Model 1. Cross sections of the velocity (a) and anomalous density (b) distributions obtained by separate inversions of seismic and gravity data.

Then we run the joint inversion of the seismic and gravity data using the Gramian constraints. The stopping criterion for the misfit level was set at 1%.

Figure 3 shows the joint inversion result for the (a) seismic data and (b) gravity data, where the white boxes show the location of the two anomalous bodies. One can see that the results of joint inversion demonstrate a significant improvement in imaging the density distribution.

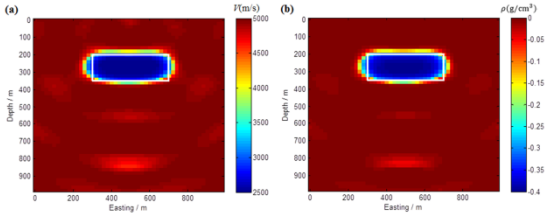

Figure 3: Model 1. Cross sections of the velocity (a) and anomalous density (b) distributions obtained by joint inversion of seismic and gravity data using Gramian constraints. The white boxes outline the true location of the anomalous body.

Model 2: SEG salt dome model

In the second numerical study we have used synthetic seismic and gravity data computer simulated for the 3D SEG salt dome model. Since the original SEG salt model has a huge number of cells, 670 × 670 × 210, we reduced the number of discretization cells into 112 × 112 × 70, by increasing the cell size to 50 m ×50 m ×25 m. The synthetic correlation between the densities ρ and velocity v can be described by Gardner's equation (4) with (k, l)=(0.31, 0.25). We considered the full SEG salt dome model, which contains not only the salt body but some other geological features, e.g. geological faults. In this test, the synthetic observed seismic and gravity FTG data were all contaminated by 3% Gaussian noise. We applied Ricker wavelet with a peak frequency of 20 Hz for the seismic source term. The frequencies used for this synthetic study were 1 Hz, 2.5 Hz and 5 Hz. The FTG components used in this model study were G_{zz}, G_{zx}, G_{zy}, G_{xx}, G_{yy}, and G_{xy}. Both the seismic and gravity inversions reached the misfit level of 3%. First, we ran separate inversions for the seismic data and the gravity FTG data. Figures 4 and 5, panels (a) and (b) show the vertical cross sections of the synthetic density and velocity models along the profiles at Y=3000 m and Y=4000 m, respectively, where panels (c) and (d) present the separate inversion results for the gravity FTG and seismic data. As one can see, the gravity inversion recovered the background features of the model well, while the seismic inversion located the salt body better than the background. Figure 6 shows a cross plot between the inverse density and velocity in the logarithmic space obtained by the separate inversions.

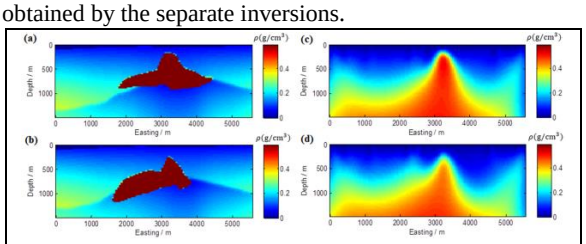

Figure 4: SEG salt model. Cross sections of the anomalous density distributions obtained by separate inversion of gravity data. Panels (a) and (b) show the true cross sections of the synthetic density model at Y=3000 m and Y=4000 m, respectively. Panels (c) and (d) show the results obtained by separate inversion of the FTG data.

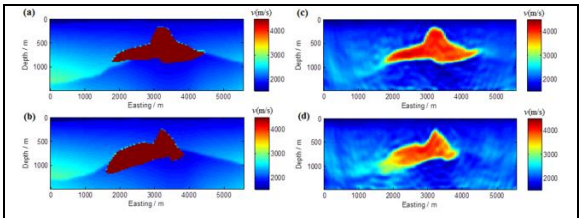

Figure 5: SEG salt model. Cross sections of the velocity distributions obtained by separate inversion of seismic data. Panels (a) and (b) show the true cross sections of the velocity model at Y=3000 m and Y=4000 m, respectively. Panels (c) and (d) show the results obtained by separate inversion of the seismic data.

Then, we ran the joint inversion with Gramian constraints. The joint inversion converged to the misfit level of 3%. Figures 7 and 8, panels (a) and (b), show the corresponding cross sections of the density and velocity distributions of the SEG salt model at Y=3000 m and Y=4000 m, respectively. Panels (c) and (d) present the results of the joint inversion of gravity FTG and seismic data using Gramian constraint. Obviously, the joint inversion has combined the advantages of the seismic and gravity inversions. It is clear that the salt body was recovered well, as well as some of the fault features and the variations of the background. Figure 9 presents a cross plot between the density and velocity in the logarithmic space versus the straight line representing the Gardner's equation, which indicates a good model correlation.

© 2017 SEG

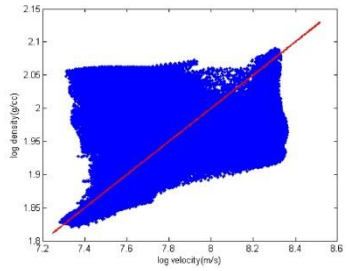

Figure 6: SEG salt model. Cross plot between the log density and velocity obtained by separate inversions. The red line indicates the linear correlation according to Gardner's equation.

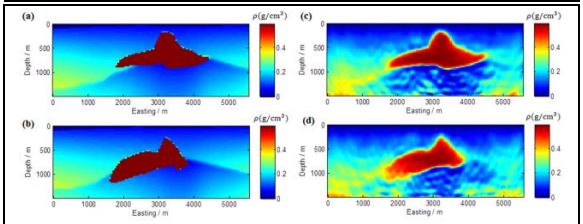

Figure 7: Panels (a) and (b) show the true cross sections of the synthetic density model at Y=3000 m and Y=4000 m, respectively. Panels (c) and (d) show the results obtained by the joint inversion.

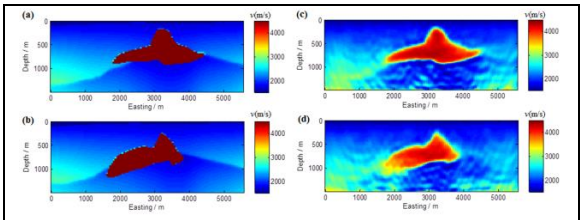

Figure 8: SEG salt model. Panels (a) and (b) show the true cross sections of the synthetic velocity model at Y=3000 m and Y=4000 m, respectively. Panels (c) and (d) show the results obtained by the joint inversion.

The results of these model studies indicate that the developed joint inversion takes into account the existence of empirical linear relationships between the log density and the log seismic velocity, and uses this relationship in the construction of the corresponding Gramian stabilizer. However, the developed algorithm does not require a priori knowledge of the specific parameters of the correlation between the density and velocity. In fact, this algorithm provides the means to find these parameters from the inversion without actual measurement of the physical properties of the rock samples by determining the parameters of the linear regression in the corresponding cross plots of log density and log velocity.

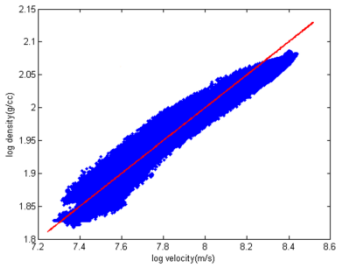

Figure 9: SEG salt model. Cross plot between the log density and velocity obtained by the joint inversions. The red line indicates the linear correlation according to Gardner's equation.

Conclusion

We have developed a method of joint inversion of the seismic and gravity gradiometry data based on the concept of a Gramian stabilizer. The Gramian enforces the linear relationships between the different model parameters and their attributes or transforms. Considering that the seismic velocity and density are related by Gardner's empirical equation, which provides a linear relationship on logarithmic scales, we incorporated this empirical rule in the joint inversion via a Gramian functional of log velocity and density. The important difference between the Gramian approach to the joint inversion from the conventional method based on the known form of correlations between, e.g., density and velocity, is that the former does not require knowing a priori a specific form of these relationships. Moreover, one can find the empirical equation between the different model parameters based on the results of the joint inversion, and without conducting petrophysical measurements on the rock samples.

We have tested the developed method and computer code of joint inversion using a synthetic model study, which included a complicated SEG model of the salt dome structure located in a complex environment. The results of the model study confirm the effectiveness of the developed approach. Future research will be aimed at application of this novel method to joint inversion of the field seismic and gravity gradiometry data.

Acknowledgements

This research was supported by the RSF grant, project No. 16-11-10188. The authors also acknowledge support from the University of Utah's Consortium for Electromagnetic Modeling and Inversion (CEMI) and TechnoImaging.

We would like to thank Mr. Shihang Feng and Dr. Yue Zhu for valuable suggestions.

Downloaded 09/12/17 to 155.101.18.153. Redistribution subject to SEG license or copyright; see Terms of Use at http://library.seg.org/

© 2017 SEG

Downloaded 09/12/17 to 155.101.18.153. Redistribution subject to SEG license or copyright; see Terms of Use at http://library.seg.org/

EDITED REFERENCES

Note: This reference list is a copyedited version of the reference list submitted by the author. Reference lists for the 2017 SEG Technical Program Expanded Abstracts have been copyedited so that references provided with the online metadata for each paper will achieve a high degree of linking to cited sources that appear on the Web.

REFERENCES

Aki, K., and P. G. Richards, 1980, Quantitative seismology: W. R. Freeman and Co.

Bleistein, N., 1984, Mathematical methods for wave phenomena: Academic Press Inc.

Brekhovskikh, L. M., 1980, Waves in layered media (2nd ed.): Academic Press Inc.

Chen, J., G. M. Hoversten, D. Vasco, Y. Rubin, and Z. Hou, 2007, A Bayesian model for gas saturation estimation using marine seismic AVA and CSEM data: Geophysics, **72**, no. 2, WA85–WA95, https://doi.org/10.1190/1.2435082.

Colombo, D., and M. De Stefano, 2007, Geophysical modeling via simultaneous joint inversion of seismic, gravity, and electromagnetic data: Application to prestack depth imaging: The Leading Edge, **26**, 326–331, https://doi.org/10.1190/1.2715057.

Dell'Aversana, P., 2013, Cognition in geosciences — The feeding loop between geo-disciplines, cognitive sciences and epistemology: EAGE Publications, 204.

Gallardo, L. A., and M. A. Meju, 2003, Characterization of heterogeneous near-surface materials by joint 2D inversion of DC resistivity and seismic data: Geophysical Research Letters, **30**, 1658–1661, https://doi.org/10.1029/2003gl017370.

Gallardo, L. A., and M. A. Meju, 2004, Joint two-dimensional DC resistivity and seismic travel time inversion with cross-gradients constraints: Journal of Geophysical Research, **109**, B03311, https://doi.org/10.1029/2003jb002716.

Gallardo, L. A., and M. A. Meju, 2007, Joint two-dimensional cross-gradient imaging of magnetotelluric and seismic traveltime data for structural and lithological classification: Geophysical Journal International, **169**, 1261–1272, https://doi.org/10.1111/j.1365-246x.2007.03366.x.

Gallardo, L. A., and M. A. Meju, 2011, Structure-coupled multiphysics imaging in geophysical sciences: Reviews of Geophysics, **49**, RG1003, https://doi.org/10.1029/2010rg000330.

Gardner, G. H. F., L. W. Gardner, and A. R. Gregory, 1974, Formation velocity and density — The diagnostic basics for stratigraphic traps: Geophysics, **39**, 770–780, https://doi.org/10.1190/1.1440465.

Haber, E., and D. Oldenburg, 1997, Joint inversion: A structural approach: Inverse Problems, **13**, 63–67, https://doi.org/10.1088/0266-5611/13/1/006.

Lippmann, B. A., and J. Schwinger, 1950, Variational principles for scattering processes. I: Physical Review Letters, **79**, 469–480, https://doi.org/10.1103/physrev.79.469.

Vozoff, K., and D. L. B. Jupp, 1975, Joint inversion of geophysical data: Geophysical Journal of the Royal Astronomical Society, **42**, 977–991, https://doi.org/10.1111/j.1365-246x.1975.tb06462.x.

Zhdanov, M. S., 2002, Geophysical inverse theory and regularization problems: Elsevier.

Zhdanov, M. S., 2015, Inverse theory and applications in geophysics: Elsevier.

Zhdanov, M. S., A. V. Gribenko, and G. Wilson, 2012a, Generalized joint inversion of multimodal geophysical data using Gramian constraints: Geophysical Research Letters, **39**, L09301, 1–7, https://doi.org/10.1029/2012gl051233.

Zhdanov, M. S., A. V. Gribenko, G. Wilson, and C. Funk, 2012b, 3D joint inversion of geophysical data with Gramian constraints: A case study from the Carrapateena IOCG deposit, South Australia: The Leading Edge, **31**, 1382–1388, https://doi.org/10.1190/tle31111382.1.